Textures and Microstructures, 1988, Vols. 8 & 9, pp. 173–189
Reprints available directly from the publisher
Photocopying permitted by license only

Printed in the United Kingdom

Effect of Ti on the Development of Rolling Textures in High Purity Iron

HIROSUKE INAGAKI

Technical Research Center, Nippon Kokan K.K., 210 Kawasaki-shi, Kawasaki-ku, Minamiwatarida-chou 1-1, Japan

(Received 3 July 1987)

Dedicated to the memory of Professor Günter Wassermann

With the method of the crystallite orientation distribution function analysis, the development of the rolling texture was studied in detail on a Fe-0.004%C-0.20%Ti alloy cold rolled up to 90% reduction in thickness. It was found that the effect of Ti was widely different among various rolling texture components. The addition of Ti enhanced the development of the ⟨110⟩||RD fiber rolling texture component by promoting the rotation about the ⟨110⟩||RD axis. This resulted in the development of the strong {112}⟨110⟩ texture component. As to the ⟨110⟩||TD fiber texture component, it was found that, although the addition of Ti did not affect the rotation about the ⟨110⟩||TD axis in the range {110}⟨001⟩ to {554}⟨225⟩, it strongly suppressed the rotation of {554}⟨225⟩ into {111}⟨112⟩. As a result, strong {554}⟨225⟩ rolling texture component was developed below 70% rolling reduction. This component seems to provide origins of the {554}⟨225⟩ recrystallization texture commonly observed in the Ti-stabilized steel. Such changes in the rolling texture would be expected, since slip modes are strongly affected by scavenging of C atom by Ti, or by the presence of very fine TiC precipitate particles.

KEY WORDS: Rolling texture, ODF-analysis, iron, titanium-alloyed, crystal rotation.

1 INTRODUCTION

It is well known that the addition of Ti greatly enhances the development of the {111} recrystallization texture in low carbon steels. As possible explanations for this, it has been thought that

solute Ti atoms (Goodenow and Held, 1970), precipitation of the TiC particles (Matsuo and Takahashi, 1971, Fukuda and Shimizu, 1972, 1975) and scavenging of C atoms by Ti (Kokubo *et al.*, 1973) play important roles in the formation of the recrystallization texture.

On the other hand, rather little attention had been directed to the effect of Ti on the development of the cold rolling texture (Willis *et al.*, 1975, Matsuo *et al.*, 1972 and V. Schlippenbach *et al.*, 1986). Since this effect might not be so pronounced as to be readily detected by the conventional pole figure method, more reliable and quantitative methods of the texture analysis should be adopted. By using the method of the three dimensional crystallite orientation distribution function analysis (Bunge, 1969), it has been found that the addition of Ti enhances the development of the $\{112\}\langle 110\rangle$ component in the cold rolling texture (Willis *et al.*, 1975, Matsuo *et al.*, 1972, V. Schlippenbach *et al.*, 1986). In most cases, this has been attributed to the presence of rather strong $\{112\}\langle 110\rangle$ transformation textures in hot bands (Willis *et al.*, 1975 and V. Schlippenbach *et al.*, 1986), and contributions of other factors have not been clarified as yet.

Also rolling reductions adopted in the previous investigations have been limited between 70 (Willis *et al.*, 1975 and Matsuo *et al.*, 1972) and 80% (V. Schlippenbach *et al.*, 1986), and the effect of rolling reductions has not been studied systematically as yet. For this reason, it is not clear at present how the crystal rotation which occurs during cold rolling is affected by the addition of Ti.

In the previous paper (Inagaki, 1987), it has been found in a 0.05%C rimmed steel that the path of this crystal rotation consists of following two branches, i.e., (i) $\{110\}\langle 001\rangle \rightarrow \{554\}\langle 225\rangle \rightarrow \{111\}\langle 112\rangle \rightarrow \{111\}\langle 110\rangle \rightarrow \{332\}\langle 011\rangle$ and (ii) $\{100\}\langle 001\rangle \rightarrow \{100\}\langle 011\rangle \rightarrow \{211\}\langle 011\rangle \rightarrow \{322\}\langle 011\rangle$, both leading to the common $\{322\}\langle 011\rangle$ stable end orientation.

In this investigation, it was tried to clarify how the rate of rotation along these two pathes was affected by the addition of Ti. The influence of the transformation texture was eliminated by using hot bands having weak transformation textures. The effect of the transformation texture on the development of the cold rolling texture was independently evaluated by using hot bands in which strong transformation textures were developed by controlled rolling.

2 EXPERIMENTS

The starting materials used in the present investigation were 150 kg ingots of high purity Fe-0.004%C-0.20%Ti and Fe-0.023%C-0.13%Ti alloys, both melted in a vacuum induction furnace. Contents of other elements were Mn, 0.35%, P, 0.002%, S, 0.001% and Al, 0.032%, respectively. Fe-0.004%C-0.20%Ti alloy was used to investigate the effect of Ti on the rate of the crystal rotation which occurs during cold rolling. After slabing, the ingot of this alloy was hot rolled to the thickness of 3 mm. In order to avoid the development of the strong transformation texture, hot rolling was finished at 930°C. After pickling, the hot bands were cold rolled to 50, 70 and 90% reduction in thickness. Specimens cut from these cold rolled sheets were chemically thinned down to 0.05 mm thickness. From the {110}, {200} and {211} pole figures determined on these specimens, crystallite orientation distribution functions were calculated with the method of Roe up to $l = 22$. By comparing orientation distribution functions observed at each rolling reductions with those of the 0.05%C rimmed steel (Inagaki, 1987), the effect of Ti addition on the crystal rotation was quantitatively evaluated.

The effect of the transformation texture on the development of the cold rolling texture was investigated on Fe-0.023%C-0.13%Ti alloy. By controlled rolling (Inagaki, 1984) this alloy with the finishing temperature of 850°C, 3 mm thick hot bands having strong transformation textures could be prepared. This alloy was cold rolled 70% reduction in thickness. By comparing orientation distribution functons of these specimens with those of Fe-0.004%C-0.20%Ti alloy, the effect of the transformation texture was estimated.

3 RESULTS

3.1 Effect of Ti on the crystal rotation

Figure 1 illustrates $\phi = 45°$ sections of the crystallite orientation distribution functions observed in Fe-0.004%C-0.20%Ti alloy at each rolling reductions. (Positions of ideal orientations on $\phi = 45°$ sections are illustrated in detail elsewhere, Inagaki, 1987.) The hot

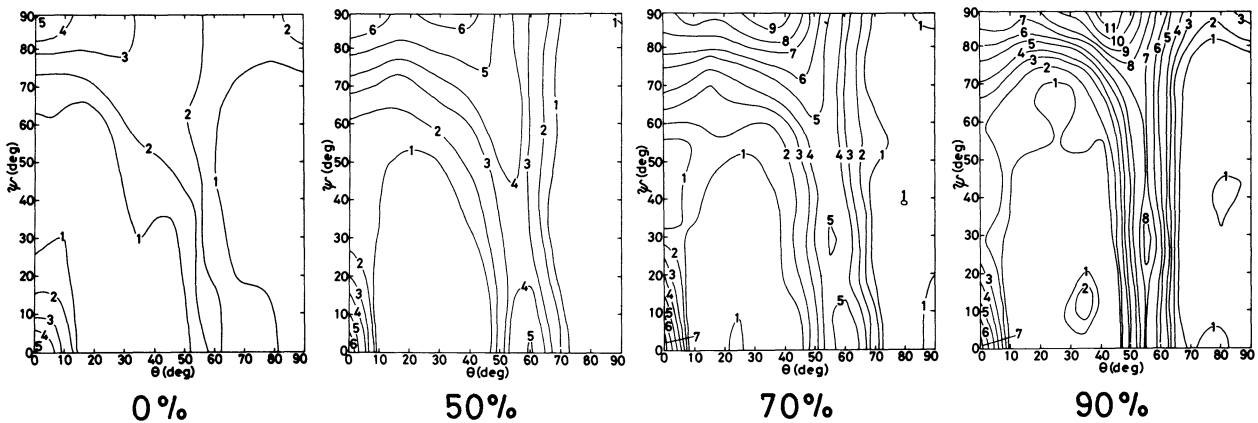

Figure 1 $\phi = 45°$ sections of the crystallite orientation distribution functions observed in Fe-0.004%C-0.20%Ti alloy after 0, 50, 70 and 90% cold rolling.

band had a rather strong $\{100\}\langle 011\rangle$ texture. However, components of transformation textures derived from the austenite rolling texture, such as $\{311\}\langle 011\rangle$ and $\{332\}\langle 113\rangle$ (Inagaki, 1977) were considerably weak. Orientation distributions observed at each rolling reductions were qualitatively the same as those observed in 0.05%C rimmed steel (Inagaki, 1987). However, intensities of textures were generally much stronger in Fe-0.004%C-0.20%Ti alloy. These features are more clearly illustrated in Figures 2, 3, 4 and 5, in which orientation distributions of Fe-0.004%C-0.20%Ti alloy are directly compared with those of the 0.05%C rimmed steel.

Figure 2 shows orientation distributions along $\psi = 90°$ lines on $\phi = 45°$ sections given in Figure 1. Orientations having the $\langle 110\rangle$ axes parallel to the rolling direction (i.e. members of the $\langle 110\rangle \| \mathrm{RD}$† fiber texture) are all located on this line. In the as hot rolled condition, Figure 2(a), this fiber texture was somewhat stronger in Fe-0.004%C-0.20%Ti alloy. However, the difference was small. After 50% rolling reduction, Figure 2(b), orientations in the range $\{100\}\langle 011\rangle$ to $\{111\}\langle 110\rangle$ showed much more remarkable development in Fe-0.004%C-0.20%Ti alloy. Between these two specimens, the difference in these components became largest at 70% rolling reduction, Figure 2(c).

At 90% rolling reduction, Figure 2(d), the difference became smaller again. However, throughout the orientation range between $(001)[\bar{1}\bar{1}0]$ and $(\bar{1}10)[\bar{1}\bar{1}0]$, all orientations were clearly much stronger in Fe-0.004%C-0.20%Ti alloy than in 0.05%C rimmed steel. Also $(\bar{2}23)[\bar{1}\bar{1}0]$ stable end orientation (Inagaki, 1987) was much more well-developed in Fe-0.004%C-0.20%Ti alloy.

From these results, it is clear that, even in the absence of the strong $\{112\}\langle 110\rangle$ component in hot bands, strong $\langle 110\rangle \| \mathrm{RD}$ fiber rolling texture, above all $\{211\}\langle 011\rangle$ rolling texture component can be developed by the addition of Ti.

Figure 3 shows orientation distributions along $\psi = 0°$ lines on $\phi = 45°$ sections given in Figure 1. All orientations having the $\langle 110\rangle$ axes parallel to the transverse direction and lying in the range $(001)[110]$ to $(\bar{1}10)[001]$ (i.e., members of the $\langle 110\rangle \| \mathrm{TD}$ fiber textures) are located on the line.

† In this paper, RD, TD and ND denote rolling, transverse and normal directions, respectively.

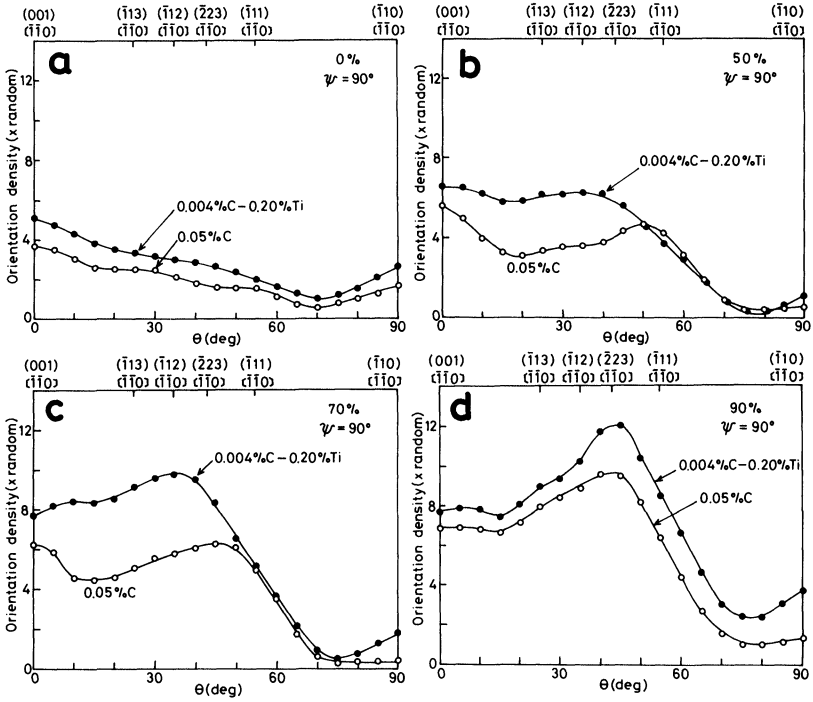

Figure 2 Orientation distributions along $\psi = 90°$ line on $\phi = 45°$ sections given in Figure 1. Rolling reductions; a) 0% (as hot rolled), b) 50%, c) 70% and d) 90%, respectively.

In the as hot rolled condition, Figure 3(a), 0.05%C rimmed steel had a uniform orientation distribution between $(\bar{1}11)[1\bar{1}2]$ and $(\bar{1}10)[001]$, whereas Fe-0.004%C-0.20%Ti alloy showed in this range a broad peak whose center was located at about $(\bar{5}54)[2\bar{2}5]$ orientation. Since orientations near $(\bar{5}54)[2\bar{2}5]$ would be derived from the Cu type rolling texture in the austenite phase via Kurdjmov-Sachs relationship (Inagaki, 1977), these results suggest that some of the austenite in Fe-0.004%C-0.20%Ti were not recrystallized. In this hot band, however, strong $(001)[\bar{1}\bar{1}0]$ and $(\bar{1}\bar{1}0)[\bar{1}\bar{1}0]$ components were also present. Since these components would be derived from the austenite recrystallization texture via

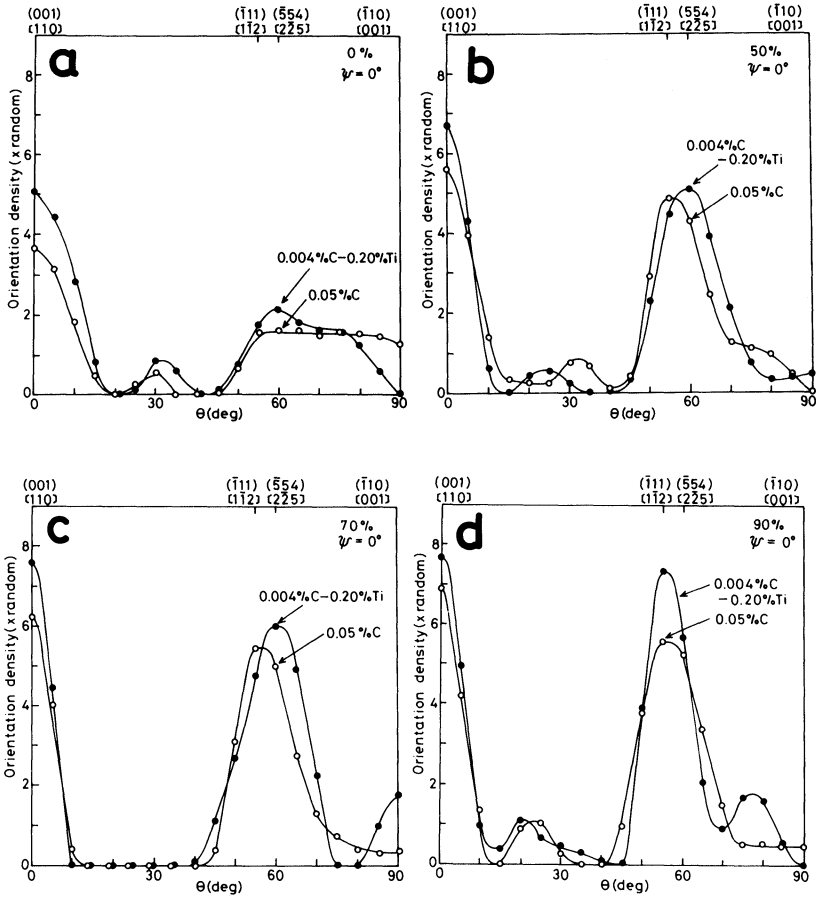

Figure 3 Orientation distributions along $\psi = 0°$ line on $\phi = 45°$ sections given in Figure 1. Rolling reductions; a) 0% (as hot rolled), b) 50%, c) 70% and d) 90%, respectively.

Kurdjmov-Sachs relationship (Inagaki 1977), it might be concluded that most of the austenite were recrystallized in this hot band.

After 50% cold rolling, Figure 3(b), crystal rotation occurred in both specimens about the $\langle 110 \rangle$ axis lying parallel to the transverse directions, forming distinct peaks at $\theta = 55$ or 60°. However, this rotation seemed to occur more readily in 0.05%C rimmed steel than

in Fe-0.004%C-0.20%Ti alloy. In the former case, the peak was located at $(\bar{1}11)[1\bar{1}2]$, whereas in the latter case, it was located at $(\bar{5}54)[2\bar{2}5]$. The height of the peak was nearly the same in both cases.

After 70% cold rolling, Figure 3(c), both peaks increased their heights appreciably. This increase was much larger in Fe-0.004%C-0.20%Ti alloy. Positions of peaks, however, did not show any change. It should be noted that $(\bar{5}54)[2\bar{2}5]$ orientation was quite stable in Fe-0.004%C-0.20%Ti alloy. In this alloy, rotation about the $\langle 110\rangle \| \mathrm{TD}$ axis beyond $(\bar{5}54)[2\bar{2}5]$ orientation seems to be strongly suppressed. Further rotation about the $\langle 110\rangle \| \mathrm{TD}$ axis toward $(\bar{1}11)[1\bar{1}2]$ occurred only after 90% cold rolling, Figure 3(d).

Figure 4 shows orientation distributions along $\theta = 55°$ line on $\phi = 45°$ sections given in Figure 1. All orientations having $\langle 111\rangle$ axes parallel to the normal direction (i.e., members of the $\langle 111\rangle \| \mathrm{ND}$ fiber texture) are located on this line. Below 70% rolling reduction, no marked difference was observed between 0.05%C rimmed steel and Fe-0.004%C-0.20%Ti alloy. In both cases, rather uniform orientation distributions were observed after 70% cold rolling, indicating the formation of the uniform $\langle 111\rangle \| \mathrm{ND}$ fiber

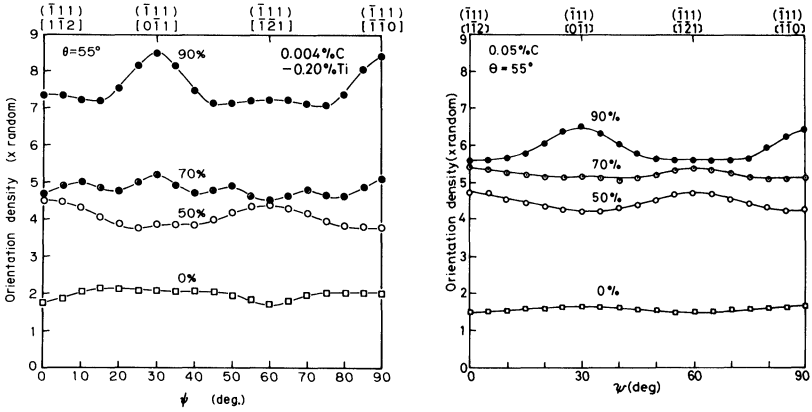

a) Fe-0.004%C-0.20%Ti alloy b) 0.05%C rimmed steel

Figure 4 Orientation distributions along $\theta = 55°$ line on $\phi = 45°$ sections given in Figure 1. a) Fe-0.004%C-0.20%Ti alloy, b) 0.05%C rimmed steel.

texture. After 90% cold rolling, {111}⟨011⟩ orientations became in both cases the main orientation among the members of the ⟨111⟩||ND fiber texture. But it should be noted in the case of Fe-0.004%C-0.20%Ti alloy that, above 70% rolling reduction, all members of the ⟨111⟩||ND fiber texture increased their intensities appreciably.

3.2 Effect of the transformation texture

In Figure 5, $\phi = 45°$ sections of the crystallite orientation distribution functions observed in hot bands of Fe-0.004%C-0.20%Ti and Fe-0.023%C-0.13%Ti alloys are compared. It is evident that crystallite orientation distribution functions are quite different between these two alloys.

This is more clearly shown in Figures 6 and 7. Figure 6 shows orientation distributions along $\psi = 90°$ line on $\phi = 45°$ sections given in Figure 5. In Fe-0.023%C-0.13%Ti alloy, a distinct peak was present at $(\bar{1}13)[\bar{1}\bar{1}0]$ orientation. $(001)[\bar{1}\bar{1}0]$ and $(\bar{1}10)[\bar{1}\bar{1}0]$ were much weaker than in Fe-0.004%C-0.20%Ti alloy.

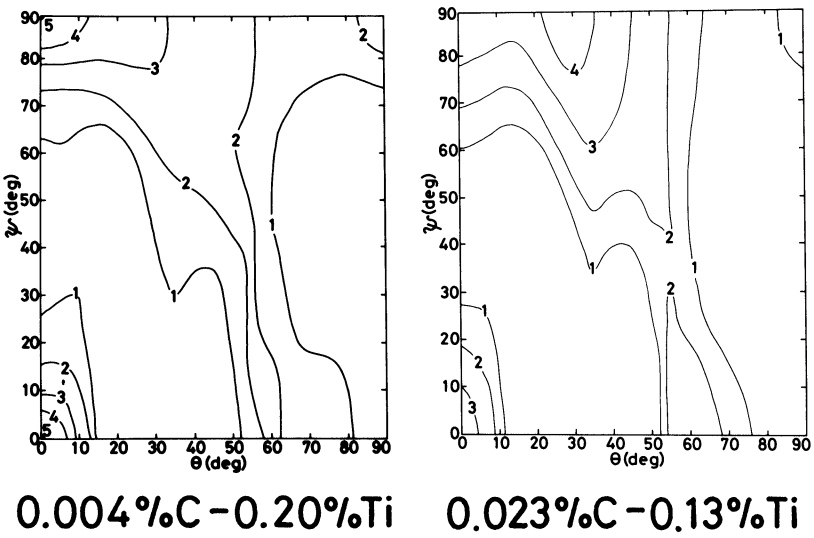

Figure 5 $\phi = 45°$ sections of the crystallite orientation distribution functions observed in the hot bands of Fe-0.004%C-0.20%Ti and Fe-0.023%C-0.13%Ti alloys.

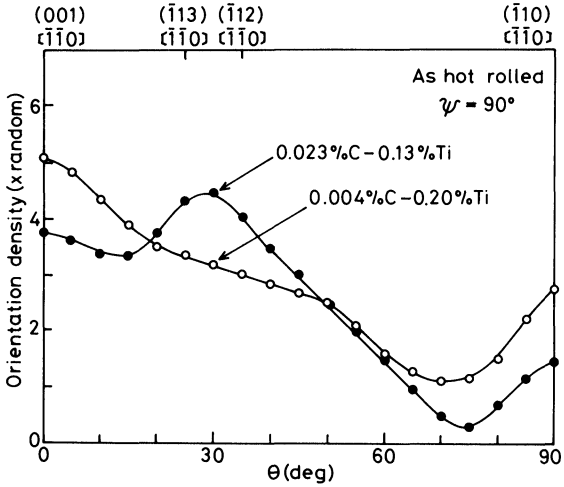

Figure 6 Orientation distributions along $\psi = 90°$ line on $\phi = 45°$ sections given in Figure 5.

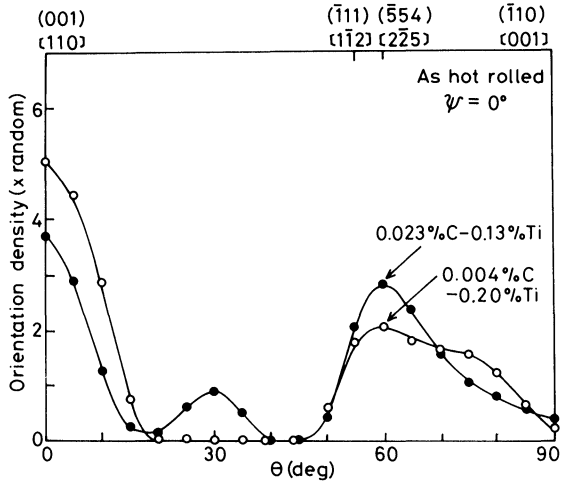

Figure 7 Orientation distributions along $\psi = 0°$ line on $\phi = 45°$ sections given in Figure 5.

Figure 7 illustrates orientation distributions along $\psi = 0°$ line on $\phi = 45°$ sections given in Figure 5. In Fe-0.023%C-0.13%Ti alloy, a strong peak was present at $(\bar{5}54)[2\bar{2}5]$ orientation.

Thus, it is evident that the hot bands of Fe-0.023%C-0.13%Ti alloy had a relatively strong texture consisting of $\{554\}\langle 225\rangle$ and $\{311\}\langle 011\rangle$ main orientations. These are components of the transformation textures derived from the Cu-type austenite rolling texture via Kurdjumov-Sachs relationship (Inagaki, 1977). In this alloy, recrystallization of the austenite might have been more effectively suppressed than in Fe-0.004%C-0.20%Ti alloy, since volume fraction of TiC particles precipitated was larger because of higher C content. In addition to this, since controlled rolling with the lower finishing temperature was adopted in hot rolling, austenite rolling texture developed in this alloy might have beeen much stronger. As a result, transformation textures inherited from these austenite rolling textures were much stronger in this alloy. Figure 8 shows $\phi = 45°$ sections of the crystallite orientation distribution functions observed after 70% cold rolling. At first glance it is clear that the rolling texture is weaker in Fe-0.023%C-0.13%Ti alloy than

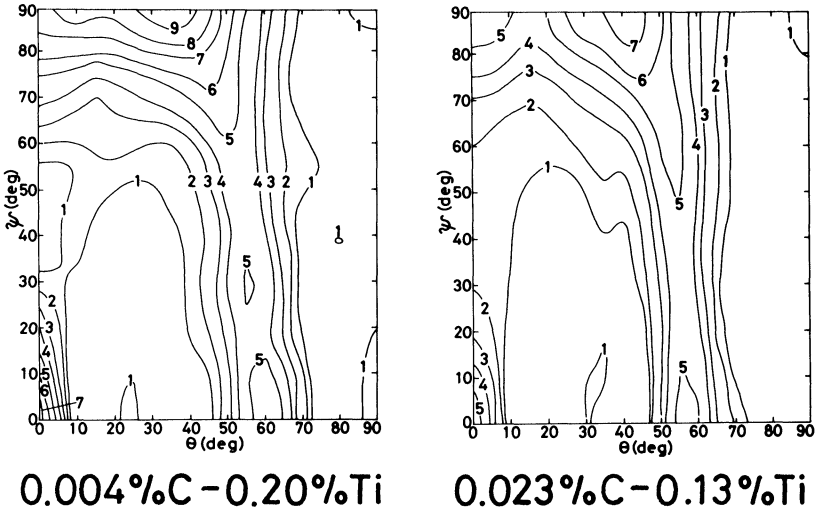

Figure 8 $\phi = 45°$ sections of the crystallite orientation distribution functions observed in Fe-0.004%C-0.20%Ti and Fe-0.023%C-0.13%Ti alloys after 70% cold rolling.

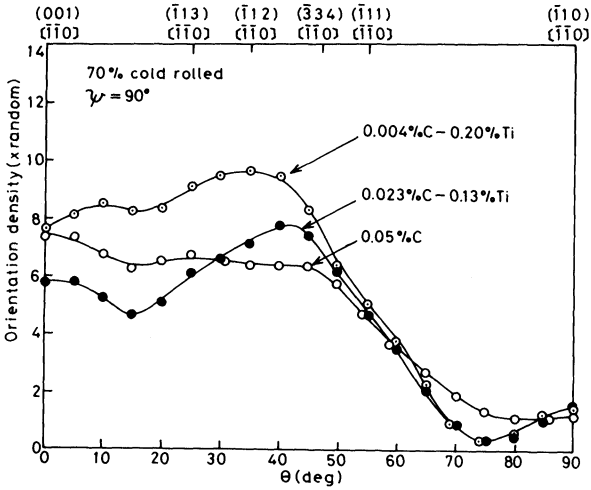

Figure 9 Orientation distributions along $\psi = 90°$ line on $\phi = 45°$ sections given in Figure 8.

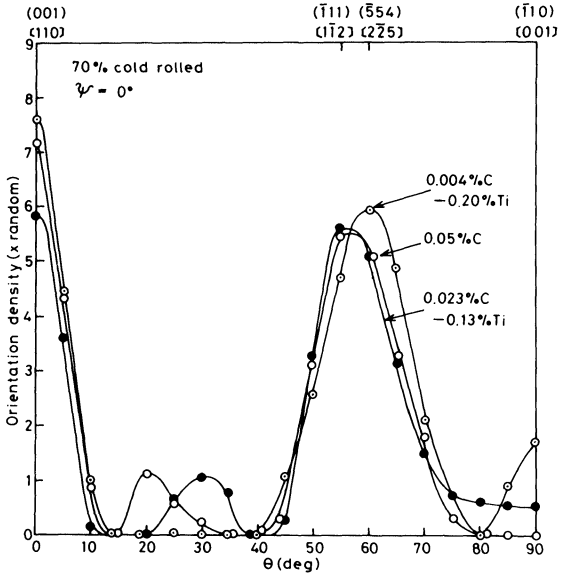

Figure 10 Orientation distributions along $\psi = 0°$ line on $\phi = 45°$ sections given in Figure 8.

in Fe-0.004%C-0.20%Ti alloy. Orientation distributions along $\psi = 90°$ line on these $\phi = 45°$ sections are shown in Figure 9. It should be noted that orientations in the range between $(001)[\bar{1}\bar{1}0]$ and $(\bar{1}11)[1\bar{1}0]$ were not well developed in Fe-0.023%C-0.13%Ti alloy. In this alloy, orientations in the range between $(001)[\bar{1}\bar{1}0]$ and $(\bar{1}\bar{1}2)[\bar{1}\bar{1}0]$ were even weaker than in 0.05%C rimmed steel.

Figure 10 shows orientation distributions along $\psi = 0°$ line on $\phi = 45°$ sections given in Figure 8. Orientation distributions in Fe-0.023%C-0.13%Ti alloy had a maximum at $(111)[1\bar{1}2]$ orientation. However, both the height and position of this maximum were the same as those observed in the 0.05%C rimmed steel.

From these results, it is evident that the addition of excess amount of C smears out the strong development of $\{112\}\langle 110\rangle$ and $\{554\}\langle 225\rangle$ rolling texture components observed in Fe-0.004%C-0.20%Ti alloy).

4 DISCUSSION

With the crystallite orientation distribution function analysis, it has already been found that the addition of Ti enhances the development of the $\{112\}\langle 110\rangle$ component of the rolling texture in low carbon steels cold rolled 70 to 80% (Willis, 1975, Matsuo *et al.*, 1972, V. Schlippenbach *et al.*, 1986). Similar observations have been made also in Nb stabilized steels (Willis *et al.*, 1975 and Hook *et al.*, 1975). Hook, Heckler and Ellias studied the effect of Nb addition on the development of the rolling texture in Fe-0.005%C alloy cold rolled 60%. They found that the $\{112\}\langle 110\rangle$ rolling texture component increased remarkably with the increasing Nb content. Since the rolling reduction adopted in these investigations have been limited between 60 and 80%, it is not clear at present how the whole rotation pathes are affected by the addition of Ti or Nb. By varying the rolling reduction in wide range and by following the rotation of various rolling texture components systematically, it was found in the present investigation that not only the development of the $\langle 110\rangle \| RD$ fiber rolling texture, but also the development of the $\langle 110\rangle \| TD$ fiber rolling texture were strongly affected by the addition of Ti. Since these effects of Ti are widely different

between these two fiber rolling texture components, they will be discussed separately below.

4.1 ⟨110⟩||RD fiber rolling texture

Development of the strong {112}⟨110⟩ component in the rolling texture of Ti and Nb steels have been attributed in the past investigations to the presence of strong {112}⟨110⟩ transformation texture in hot hands (Willis *et al.*, 1975, V. Schlippenbach *et al.*, 1986 and Hook *et al.*, 1975). It has been considered that cold rolling results in the reinforcement of this component, since it is the stable end orientation of cold rolling (Hook *et al.*, 1975). It is wellknown in the case of control-rolled low carbon microalloyed steels that such transformation textures can be developed appreciably, if recrystallization of austenite is suppressed by the precipitation of NbC or TiC, and if heavy rolling reductions are given to the unrecrystallized austenite (Inagaki, 1977). The austenite rolling texture developed through this processing is supposed to be Cu type, and the main orientations of the transformation texture derived from this austenite rolling texture via Kurdjmov-Sachs relationship were identified, in the case of 0.1%C-1.3%Mn-0.04%Nb steel, to be {311}⟨011⟩ and {322}⟨113⟩ (Inagaki, 1977). Although previous investigations have identified one of the main orientations of the transformation texture as {211}⟨011⟩, {311}⟨011⟩ seems to be better description of this component. This is also evident from Figure 6. In very low C steel, {332}⟨113⟩ component seems to be better described as {554}⟨225⟩. This is also evident from Figure 7, although spread of orientation distribution about this orientation is large.

It is readily understood that strong {112}⟨110⟩ rolling texture component can be developed by cold rolling hot bands containing strong {311}⟨011⟩ transformation texture, since {211}⟨011⟩ and {311}⟨011⟩ are only 10° apart, and since {211}⟨011⟩ is located on the rotation path toward the {322}⟨011⟩ stable end orientation (Inagaki, 1987). In the case of Fe-0.004%C-0.20%Ti alloy, however, {311}⟨011⟩ transformation texture component was not well developed in hot bands, Figures 2 and 6, since finishing temperature of hot rolling was intentionally selected to be above the recrystallization temperature of the austenite. In spite of this,

development of the strong {112}⟨110⟩ rolling texture component could be observed in this alloy cold rolled above 50% reduction in thickness. Development of the strong {112}⟨110⟩ rolling texture component cannot be explained therefore with the mechanism described above. It seems that either absence of solute carbon atom, or presence of fine TiC or NbC particles in hot bands enhances the slip rotation which results in the development of the strong {112}⟨110⟩ rolling texture component.

In ultra low carbon Ti stabilized steels, it has been confirmed that very fine TiC particles are already precipitated in hot bands (Matsuoka and Takahashi, 1971, Fukuda and Shimizu, 1972). Also, the results of internal friction measurements have indicated that solute C atoms are absent in these hot bands due to the scavenging effect of Ti atom (Fukuda and Shimizu, 1972).

In the case of Fe-0.023%C-0.13%Ti alloy, it is interesting to note that, although strong {311}⟨011⟩ transformation texture component was developed in the hot band, ⟨110⟩||RD fiber rolling texture observed after 70% rolling was quite weak. It has been observed that, in Ti stabilized steel with higher C content, TiC particles precipitated in the hot band are relatively coarse (Matsuoka and Takahashi, 1971). Presence of these coarse particles might have randomized the cold rolling texture.

From these results, it might be concluded that, although the presence of {311}⟨011⟩ transformation texture component in the hot band may be favourable to the development of {112}⟨110⟩ component in the rolling texture, it is not a necessary condition, at least at higher rolling reductions.

4.2 ⟨110⟩||TD fiber rolling texture

From Figure 3, it is clear that, in Fe-0.004%C-0.20%Ti alloy, the rotation of crystals from {554}⟨225⟩ to {111}⟨112⟩ orientations was strongly suppressed below 70% rolling reduction. As a result, a strong stable peak was formed at the {554}⟨225⟩ orientation. Since crystals in this orientation would be severely strained, it is expected that, on annealing these specimens, strong {554}⟨225⟩ recrystallization texture would be developed. This is in fact just what has been observed (Willis *et al.*, 1975, V. Schlippenbach *et al.*, 1986, Akisue and Takashima, 1973). The mechanism through which

the rotation of the {554}⟨225⟩ orientation into the {111}⟨112⟩ orientation is suppressed, is not clear at present. However, presence of very fine TiC precipitate particles seems to play here an important role.

Above 70% rolling reduction, such barrier to the crystal rotation from {554}⟨225⟩ to {111}⟨112⟩ was completely eliminated, and since all of these strong {554}⟨225⟩ orientations are rotated into {111}⟨112⟩, and further into {111}⟨110⟩ orientations, ⟨111⟩||ND fiber texture which is much stronger than that observed in the 0.05%C rimmed steel was developed.

Thus, it might be concluded that, below 70% rolling reduction, the addition of Ti enhances the development of the {554}⟨225⟩ orientation by suppressing the rotation of the {554}⟨225⟩ orientation into the {111}⟨112⟩ orientation.

In Fe-0.023%C-0.13%Ti alloy, however, such effect of Ti could not be observed. This might be also ascribed to the large amount of coarse TiC particles precipitated in the hot band of this alloy.

5 CONCLUSIONS

The addition of Ti significantly affects the development of the rolling texture in high purity iron. This effect is widely different among various components of the rolling texture.

(1) ⟨110⟩||RD fiber rolling texture components; The addition of Ti enhances the rotation of these components about the ⟨110⟩11RD axis. This leads to the development of the strong {112}⟨110⟩ rolling texture component.

(2) ⟨110⟩||TD fiber rolling texture components; In the orientation range between {110}⟨001⟩ and {554}⟨225⟩, the addition of Ti does not significantly affect the rotation of these components about the ⟨110⟩||TD axis. However, the rotation of the {554}⟨225⟩ orientation into the {111}⟨112⟩ orientation is strongly suppressed by the addition of Ti. This results in the development of the strong {554}⟨225⟩ rolling texture component.

Thus, the rolling texture of the Ti-stabilized steel can be characterized by the strong {554}⟨225⟩ and {112}⟨110⟩ components.

References

1. Akisue, O. and Takashina, K. (1973) *Trans. Japan Inst. Metals,* **14,** p. 489.
2. Bunge, H. J. (1969) *Mathematische Methoden der Texturanalyse,* Akademie Verlag, Berlin.
3. Emren, F., Von Schlippenbach, U. and Lücke, K. (1986) *Acta Metall,* **34,** p. 2105.
4. Fukuda, N. and Shimizu, M. (1972) *Sosei-to-Kakou,* **13,** p. 841.
5. Fukuda, N. and Shimizu, M. (1975) *Tetsu-to-Hagane,* **61,** p. 817.
6. Goodenow, R. H. and Held, J. F. (1970) *Metal Trans.,* **1,** p. 2507.
7. Hook, R. E., Heckler, A. J. and Ellias, A. J., (1975) *Metal. Trans.,* **6A,** p. 1683.
8. Inagaki, H. (1977) *Trans. Iron Steel Inst. Japan,* **17,** p. 166.
9. Inagaki, H. (1984) *Zeit. Metallkunde,* **75,** p. 510.
10. Inagaki, H. (1987) *Zeit. Metallkunde,* **78,** No. 6, p. 431.
11. Karlyn, D. A., Vieth, R. W. and Forand, J. L. (1969) *Mechanical Working and Processing,* AIME, New York, **VII,** p. 127.
12. Kokubo, I., Sudo, M., Kameno, M., Hashimoto, S., Tsukatani, I. and Iwai, T., (1973) *Tetsu-to-Hagane,* **59,** p. 469.
13. Matsuo, M., Hayami, S. and Tani, S. (1972) *Seitetsu Kenkyu,* **276,** p. 10207.
14. Matsuoka, T. and Takahashi, M. (1971) *Tetsu-to-Hagane,* **57,** p. 1134.
15. Roe, R. J. (1965) **36,** p. 2024.
16. Von Schlippenbach, U., Emren, F. and Lücke, K. (1986) *Acta Metall.* **34,** p. 1289.
17. Suzuki, T., (1984) Proc. 7th Int. Conf. on *Texture of Materials,* Netherlands Soc. for Material Science, p. 439.
18. Terasaki, F. and Kaneko, T. (1972) *Tetsu-to-Hagane,* **58,** p. 1674.
19. Willis, D. J., Hocking, K. and Harthley, M. (1975) *J. of Australian Inst. Metals,* **20,** p. 101.